Proceedings of the Forty-First Turbomachinery Symposium
September 24-27, 2012, Houston, Texas

STEADY STATE PERFORMANCE PREDICTION OF DIRECTLY LUBRICATED FLUID FILM JOURNAL BEARINGS

Minhui He
Machinery Specialist
BRG Machinery Consulting, LLC
Charlottesville, Virginia, USA

James M. Byrne
Machinery Specialist
BRG Machinery Consulting, LLC
Charlottesville, Virginia, USA

C. Hunter Cloud
President
BRG Machinery Consulting, LLC
Charlottesville, Virginia, USA

José A. Vázquez
Machinery Consultant
BRG Machinery Consulting, LLC
Wilmington, Delaware, USA

Minhui He is a Machinery Specialist with BRG Machinery Consulting LLC, in Charlottesville, Virginia. His responsibilities include vibration troubleshooting, rotordynamic analysis, as well as bearing and seal analysis and design. He is also conducting research on rotordynamics and hydrodynamic bearings.

Dr. He received his B.S. degree (Chemical Machinery Engineering, 1994) from Sichuan University. From 1996 to 2003, he conducted research on fluid film journal bearings in the ROMAC Laboratories at the University of Virginia, receiving his Ph.D. (Mechanical and Aerospace Engineering, 2003).

James M. Byrne is a member of the BRG Machinery Consulting team, in Charlottesville, Virginia. BRG performs research and analysis in the fields of fluid film bearings, magnetic bearings, and rotordynamics. Mr. Byrne began his career designing internally geared centrifugal compressors for Carrier in Syracuse, New York. He continued his career at Pratt and Whitney aircraft engines and became a technical leader for rotordynamics. Later Mr. Byrne became a program manager for Pratt and Whitney Power Systems managing the development of new gas turbine products. From 2001 to 2007, he was President of Rotating Machinery Technology, a manufacturer of tilting pad bearings.

Mr. Byrne holds a BSME degree from Syracuse University, an MSME degree from the University of Virginia, and an MBA from Carnegie Mellon University.

C. Hunter Cloud is President of BRG Machinery Consulting, LLC, in Charlottesville, Virginia, a company providing a full range of rotating machinery technical services. He began his career with Mobil Research and Development Corporation in Princenton, NJ, as a turbomachinery specialist responsible for application engineering, commissioning, and troubleshooting for production, refining and chemical facilities. During his 11 years at Mobil, he worked on numerous projects, including several offshore gas injection platforms in Nigeria as well as serving as reliability manager at a large US refinery.

Dr. Cloud received his BS (Mechanical Engineering, 1991) and Ph.D. (Mechanical and Aerospace Engineering, 2007) from the University of Virginia. He is a member of ASME, the Vibration Institute, and the API 684 rotordynamics task force.

José Vázquez is a Machinery Consultant at BRG Machinery Consulting, LLC. He has over 22 years of experience in machinery analysis and troubleshooting. His career started in Venezuela as a faculty member at the Universidad Simón Bolivar where he taught courses in kinematics, machinery dynamics and instrumentation, as well as some independent consulting in machinery vibration. From 1992 to 2001, he worked as lab engineer and research scientist at the Rotating Machinery and Controls (ROMAC) Laboratories at the University of Virginia, providing technical support to member companies and developing rotordynamics and bearing analysis computer programs. Prior to joining BRG, he worked for 10 years at DuPont as a Mechanical Consultant, primarily solving machinery problems and developing advanced measurement techniques.

Dr. Vázquez received his B.S. (Mechanical Engineering, 1990) and MS (Specialization in Rotating Equipment, 1993) from the Universidad Simón Bolívar in Venezuela. He received his Ph.D. (Mechanical and Aerospace Eng., 1999) from the University of Virginia. He is a member of ASME.

ABSTRACT

Predicting the performance of directly lubricated bearings is a challenge facing bearing manufacturers and end users alike. In this study, thermoelastohydrodynamic (TEHD) theories are applied to analyze three directly lubricated bearings that have been experimentally investigated by the Turbomachinery Laboratory at Texas A&M University, including two inlet groove bearings and one spray bar bearing. The main aspects of the TEHD models are presented, including an extensive discussion on groove mixing. Comparisons are made between the theoretical and experimental results for the pad temperatures and shaft centerline locations. The results, which show generally good agreement, indicate that the TEHD theories are capable of predicting the steady state performance of these directly lubricated bearings with reasonable accuracy. Limitations of the simple groove mixing model and the elastic model were also identified.

INTRODUCTION

The performance of a fluid film bearing can be categorized as steady state and dynamic. The steady state performance includes the minimum film thickness, maximum temperature and friction power loss. These parameters mainly indicate the health of the bearing itself. For example, for reliable operation, the minimum film thickness and the maximum temperature must meet certain requirements (Martin and Garner, 1973). Overly high temperature could lead to oil oxidation and/or Babbitt wiping. The dynamic performance refers to the fluid force acting on the rotor, and is typically represented as linearized stiffness and damping coefficients. The bearing's dynamics is an integral part of a machine's overall dynamics, greatly affecting its vibration characteristics such as critical speed, unbalance response and stability (Newkirk and Taylor, 1925).

The influence of bearing dynamics on rotor dynamics is prominent in rotating machinery, especially in high speed applications. First, a machine's critical speeds are often dictated by the stiffness of both the rotor and the bearings. Therefore, if the bearing is not properly designed, the machine may operate too close to a critical speed, resulting in high vibrations and high sensitivity to rotor unbalance. Second, damping in the rotor-bearing system mainly comes from the fluid film bearings. For many machines, adequate damping is necessary to suppress destabilizing forces in the system, such as the cross-coupling produced by the labyrinth seals in a compressor or fixed geometry bearings. If the damping is insufficient, the rotor may become unstable, exhibiting high sub-synchronous vibration. Sufficient damping is also necessary for a machine to smoothly cross its critical speeds without rubbing internal tight clearances.

Bearing performance should be fully considered in the design process of rotating machinery. For a low speed rigid rotor, fixed geometry bearings can usually provide satisfactory performance at a relatively low cost. For high speed flexible rotors, however, titling pad bearings are often required for rotor stability. If high temperature is a concern, direct lubrication may be adopted as a solution. Once the bearing type is selected, other parameters need to be determined to optimize its performance, including the number of pads, preload, pivot offset and the pad orientations relative to the load. All these decisions should be made based on accurate predictions of the bearing's performance. For instance, if the bearing temperature is under-predicted in design, high temperature in operation could lead to nuisance alarms and trips, or damage the bearing. If the required flowrate is under-predicted, the resulting lubrication system may not be able to supply enough oil to the bearing, leading to reduced load carrying capacity, increased operating temperature, and deteriorated bearing dynamics. If the bearing's dynamics is substantially off-design, the machine could experience unexpected high vibrations due to a variety of causes, such as insufficient separation margin or even self-excited rotor instability.

Modeling of fluid film bearings has been conducted for many years and achieved great success. A comprehensive analysis typically includes hydrodynamic pressure, film and pad temperatures, and pad deformations, and thus, is often called thermoelastohydrodynamic (TEHD) analysis. Other related aspects, such as cavitation and turbulence, should also be included in the process. Pinkus and Szeri gave excellent historical reviews in 1987, commemorating the centennial of fluid film bearing research. A more recent overview on bearing modeling can be found in He *et al*. (2005).

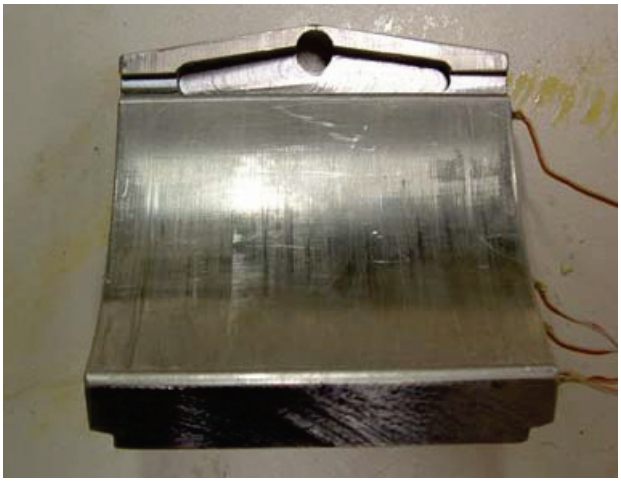

a) Inlet Groove Bearing (Courtesy Carter, 2007)

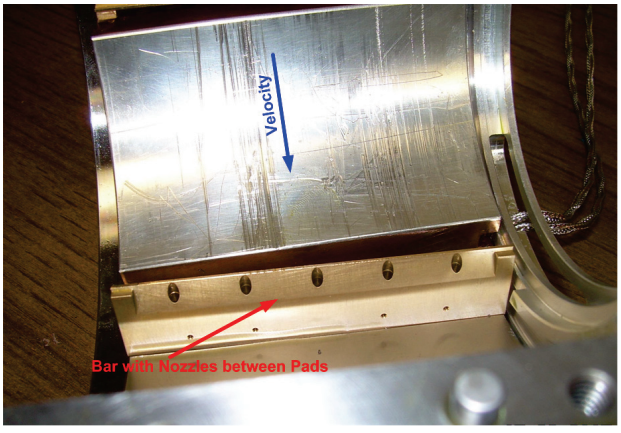

b) Spray Bar Bearing (Courtesy Harris, 2008)

Figure 1. Typical Directly Lubrication

In a conventional flooded design, oil is supplied into the bearing through orifices between pads. End seals are often installed to prevent excessive axial leakage. This design does not effectively carry cool supply oil to the inlet of each pad. Consequently, oil entering the clearance is largely the hot oil carried over from the upstream pad and the surrounding sump oil, leading to rather high temperature at the inlet. In order to achieve lower temperature, direct lubrication has become increasingly popular in recent years. The objective of direct lubrication is to maximize the cool oil being sent into the pad inlet clearance. There are generally two types of direct lubrication. The first type has an axial groove machined on the pad near its leading edge (Figure 1a). Cool oil can be sent into this groove through an oil feed tube (Mikula, 1985), or by a nozzle pointing to the inlet hole of the groove (Carter, 2007). The second type employs a bar fixed to the bearing housing with axially distributed nozzles (Figure 1b). These nozzles are typically oriented in the radial direction and their outlets are close to the shaft surface. Cool oil is sprayed towards the shaft surface in front of the pad leading edge (Sasaki *et al*., 1987). In some designs, additional supply oil is also sprayed on the back of the pad, further cooling the pad (Harris, 2008). Both types have been used and proven successful, especially in high speed applications.

Direct lubrication has been studied both experimentally and theoretically. Mikula (1985, 1988) experimentally investigated inlet groove thrust bearings. Compared to conventional designs, these directly lubricated bearings demonstrated lower temperature, reduced friction power loss and less required supply flowrate. Sasaki *et al.* (1987) tested journal and thrust bearings of the spray bar type. The spray bar bearings clearly exhibited lower temperatures. This could be simulated by reducing the hot oil carryover factor in the groove mixing model. Dmochowski *et al*. (1993) proposed a modified groove mixing model for inlet groove bearings. This model gives the cool supply oil priority to enter the thin film, resulting in reduced inlet temperature. Both theoretical and experimental results were presented and compared in their paper. Brockwell *et al.* (1994) presented the test results of several 3.875 inch (98 mm) journal bearings with various preload and pivot offset, including both inlet groove and conventional bearings. Throughout a wide operating range, the directly lubricated bearings demonstrated lower pad temperatures. These bearings could also tolerate fairly substantial flowrate reduction without causing excessive temperature rise, while reducing friction power loss. Interestingly, their test data showed that the inlet groove and its comparable conventional bearings had similar temperatures near the pad leading edges. However, the directly lubricated bearings showed much less temperature rise circumferentially along the pads, leading to lower peak temperatures downstream. Based on this observation, He *et al.* (2002) proposed an alternative explanation of the inlet groove bearing's cooling mechanism. They suggested that it was turbulence that led to the reduced temperature gradient. As shown in Figure 2, including the turbulence effects, their theoretical predictions agreed well with the test data of Brockwell *et al.* (1994). However, the mechanism that triggered turbulence was not identified. More experimental data of inlet groove bearings were presented by DeCamillo and Brockwell in 2001. Meanwhile, to understand the physics, commercial CFD software has been used to study the flow patterns inside the oil groove. Edney *et al.* (1998) studied the flow field inside the supply groove during their investigation of a rotor instability problem. Also using CFD software, Grzegorz and Michal (2007) studied the flow inside the inlet groove of a thrust bearing. Their CFD model revealed intense heat transfer between the hot oil layer and the cool oil vortices.

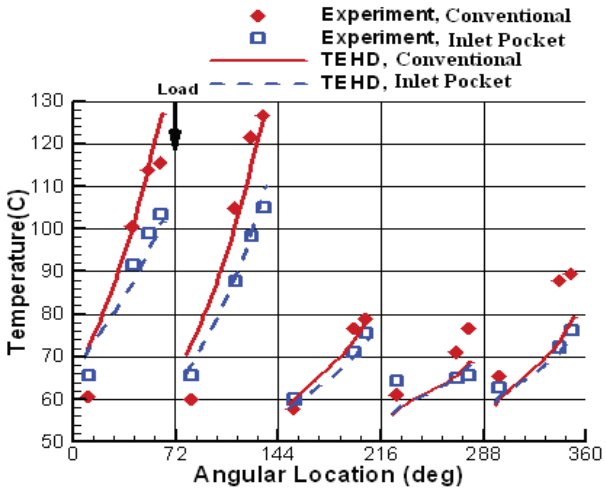

Figure 2. Pad Temperature Predictions by Triggered Turbulence, He *et al.* (2005)

Obviously, the different thermal performance of the directly lubricated bearings demands some extensions of the classic theoretical models. The objective of this study is to answer the following questions. What are the state-of-the-art techniques for modeling directly lubricated journal bearing? How well do these modeling techniques predict the steady state performance of directly lubricated bearings? What are the likely causes for these deviations between predictions and measurements?

In recent years, a series of experimental testing has been conducted at the Turbomachinery Laboratory of Texas A&M University, producing both steady state and dynamic results. In this work, the mainstream TEHD models were applied to predict the steady state performance of three directly lubricated bearings tested at Texas A&M University (Carter, 2007; Harris, 2008 and Kulhanek, 2010). These experimental works were chosen because they provide detailed experimental results on both types of direct lubrication, and all results were obtained from the same test rig, which brings some consistency across the wide range of test data.

There is no doubt that accurate prediction of the dynamic coefficients is very important. However, the confidence in the dynamic prediction is fundamentally dictated by the accuracy of the predicted steady state performance, including the journal position and pad temperatures. Therefore, the scope of this paper is limited to the modeling of steady state performance, but will be extended to cover the dynamic coefficients in the future.

MODELING ASPECTS

This section presents the theoretical models used to analyze the three directly lubricated bearings in the following order:

- General TEHD models
  - Hydrodynamic pressure
  - Film and pad temperatures
  - Elastic deformations
  - Turbulence
  - Starvation
- Groove mixing
  - Physical phenomenon
  - Classic mixing model
  - Hot oil carryover factor (λ)
  - Cool oil insertion model
  - Starvation mixing model
  - Integrated mixing model

General TEHD Models

Following the classic thermoelastohydrodynamic (TEHD) theory, the pressure is governed by the generalized Reynolds equation (Safar and Szeri, 1974).

$$\frac{\partial}{\partial x}\left\{\Gamma(x,z)\frac{\partial p}{\partial x}\right\}+\frac{\partial}{\partial z}\left\{\Gamma(x,z)\frac{\partial p}{\partial z}\right\}=-U\frac{\partial}{\partial x}G(x,z) \qquad (1)$$

This equation includes radial viscosity variation as well as turbulence. Hydrodynamic pressure is solved in the circumferential (x) and axial (z) directions, and assumed constant across the thin film (y). On the four edges of the pad, pressure equals the ambient pressure. If the pad is starved near its inlet, pressure is also specified at the ambient pressure in the starved region. If cavitation occurs, pressure is set at the cavitation pressure in the cavitated region.

Film temperature is modeled by the two-dimensional energy equation which also includes turbulent flow.

$$\rho C_p\left(u\frac{\partial T}{\partial x}+v\frac{\partial T}{\partial y}\right)=\frac{\partial}{\partial x}\left(k\frac{\partial T}{\partial x}\right)+\frac{\partial}{\partial y}\left(k_e\frac{\partial T}{\partial y}\right)+\mu_e\left[\left(\frac{\partial u}{\partial y}\right)^2+\left(\frac{\partial w}{\partial y}\right)^2\right] \qquad (2)$$

Temperature distribution varies in the circumferential (x) and radial (y) directions, but assumed constant axially (z). Physically, the film and pad temperatures are coupled together. The classic approach is to solve the heat conduction in the pad separately. Then, iteration is used to ensure that the film and pad temperatures are mutually agreeable. In this study, however, the coupled approach of Paranjpe and Han (1994) is employed. This approach solves the film and pad temperatures simultaneously, eliminating a potentially unstable iteration. For the boundary conditions, the film temperature equals the shaft temperature on the shaft surface. On the outer surfaces of the pad, a convection boundary condition is applied. At the film inlet, the film temperature is specified at the groove mixing temperature. For directly lubricated bearings, this groove mixing temperature is expected to be noticeably lower than that of conventional bearings due to their unique oil supply methods. The mixing temperature is the key subject of this study and will be discussed in the next section. The thermal boundary conditions are illustrated in Figure 3. Figure 4 shows the resulting temperature contours on the pads of a case whose probe temperatures are presented in Figure 24.

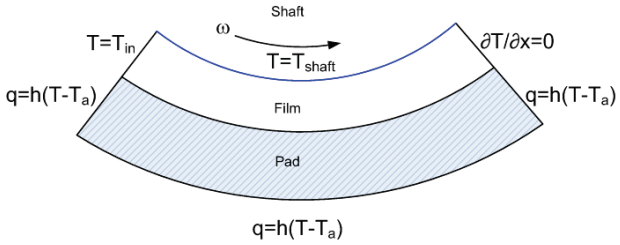

Figure 3. Thermal Boundary Conditions

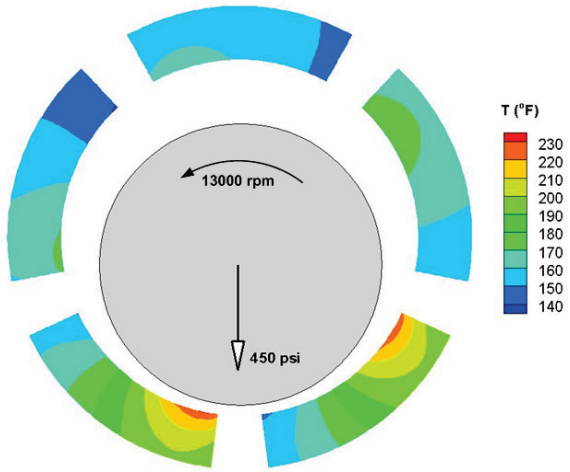

Figure 4. Example of the 2D Pad Temperature Solution

Pad mechanical and thermal deformations are calculated using two-dimensional, plain strain finite elements. Pivot flexibility is calculated based on Hertzian contact theory (Kirk and Reedy, 1988). For the shaft and bearing outer shell, the theoretical model treats them as cylinders experiencing free thermal expansion at uniform temperatures. This analytical model is rather crude considering the actual physics. For example, the shell's geometry is not as simple as a hollow cylinder, its temperature varies radially (not uniform), and it cannot freely expand since it sits inside the bearing housing.

To obtain accurate predictions, it is important to calculate the bearing's hot clearance due to thermal expansion. The hot clearance can be significantly smaller than the manufactured value, greatly affecting the bearing's performance. Since the hot clearance is physically governed by the thermal growth of the shaft, bearing pads and shell, all three components should be included in its calculation. However, in reality, since the shell condition was not sufficiently known, the calculated thermal expansion had high uncertainties that often degraded the overall hot clearance prediction. Physically, shell expansion is radially outward and acts to increase the bearing clearance. Shaft expansion is also radially outward and acts to decrease

the bearing clearance. Our inability to accurately model shell expansion led to our decision to ignore shaft expansion, as the two generally cancel each another. This simplification is not ideal, but was considered necessary. Therefore, all theoretical results presented in this study are based on hot clearances established by the pad thermal deformation only.

Turbulence is evaluated by the eddy viscosity model, which treats the added turbulent stress as the result of effectively increased fluid viscosity. This added viscosity due to turbulence (eddy viscosity) can be calculated by the Reichardt's formula (Safar and Szeri, 1974). Meanwhile, the fluctuating motion of the fluid particles in turbulent flow enhances heat transfer, leading to effectively increased thermal conductivity. Using these effective properties, the Reynolds equation and the energy equations are extended to the turbulent regime. To model flow regime transition, two critical Reynolds numbers are prescribed. The flow is laminar if the actual Reynolds number is below the lower critical number. The flow is fully turbulent if the actual Reynolds number is above the upper threshold. For transitional flow whose Reynolds number is in between, a scaling factor is applied to scale the eddy viscosity between zero and its full value (Suganami and Szeri, 1979).

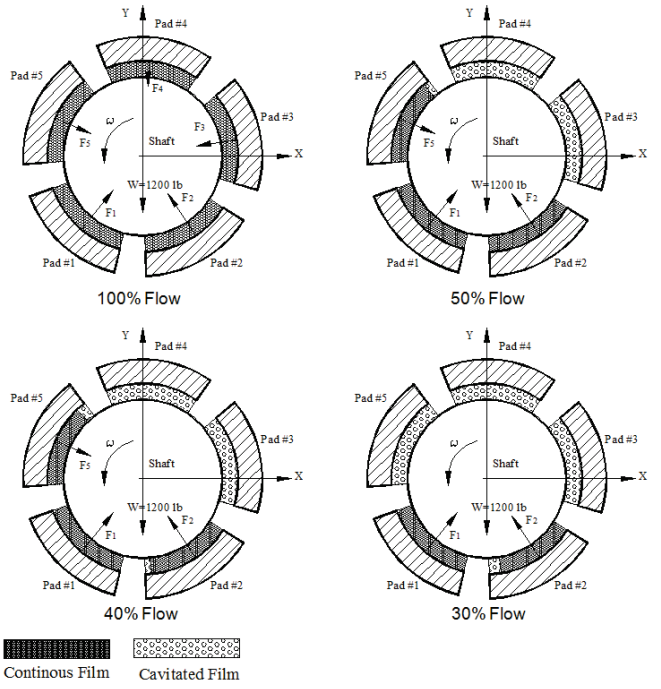

Figure 5. Development of Starvation in a 5-Pad Tilting Pad Bearing (He *et al.*, 2005)

Directly lubricated bearings are often operated in an evacuated condition in which there are no end seals. Since the bearing is not submerged in an oil bath, it is at the risk of being starved. Figure 5 schematically shows a tilting pad bearing under various levels of starvation. The oil at the pad inlet comes from the hot oil leaving the upstream pad and the cool oil out of the supply orifice. If this amount is not enough to fill the clearance at the pad leading edge, the inlet region will be starved (cavitated) and there is no hydrodynamic pressure in this region. Consequently, continuous film begins somewhere downstream where the clearance is sufficiently reduced. The task of starvation modeling is to determine the film onset location, which can be achieved by an iterative search (He *et al.*, 2005).

Groove Mixing

The mixing of hot and cool oil inside the axial groove has been studied for many years, yet remains an unsolved challenge due to its complex physics. Heshmat and Pinkus (1986) observed that, in the cavitated region, the oil is in the form of streamlets adhering to the rotating shaft surface. Even after leaving the pad trailing edge, neither the axial distribution nor the individual width of the streamlets has changed, indicating substantial hot oil carryover across the groove. Meanwhile, cool supply oil comes out of an orifice (or orifices), being distributed axially and interacting with the hot oil streamlets. The surrounding sump oil may also come into play if the bearing is flooded. Therefore, a detailed thermal and fluid analysis of the groove mixing would be extremely difficult and seems impractical at this time.

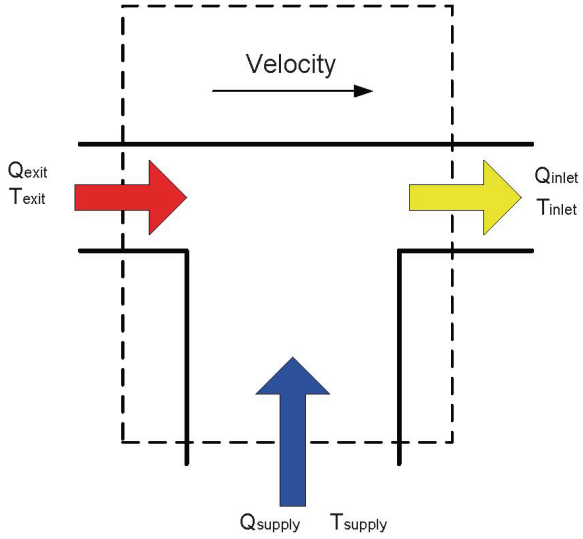

Figure 6. Groove Mixing Model Based on Energy Balance

A more practical approach is to use a simple model based on energy conservation inside the oil groove. As shown in Figure 6, the mixing temperature can be calculated according to the energy balance of the three streams assuming they are perfectly mixed.

$$T_{mix} = T_{in} = \frac{Q_{out}T_{out} + (Q_{in} - Q_{out})T_s}{Q_{in}} \tag{3}$$

In this model, the hot oil has the priority to participate in the mixing, and the amount of cool oil is subsequently determined based on flow continuity. However, the temperatures predicted by Equation (3) are often higher than the measured ones. To address the discrepancy, a hot oil

carryover factor (λ) can be introduced to modify the mixing model as following (Mitsui, *et al*, 1983).

$$T_{mix} = T_{in} = \frac{\lambda Q_{out} T_{out} + (Q_{in} - \lambda Q_{out}) T_s}{Q_{in}} \quad (4)$$

Equation (4) is the classic mixing model that is widely used in industry. The possible range of λ is between zero and one. The value of zero would completely eliminate participation of the hot oil, leading to $T_{mix} = T_s$. With the value of one, the resulting mixing temperature would be same as that given by Equation (3). λ is typically between 0.7 and 1.0 for a conventional, flooded bearing. Sasaki *et al.* (1987) used Equation (4) to model a spray bar bearing and found that λ=0.6 led to good temperature predictions. There are other alternative mixing models (Ettles and Cameron 1968, Heshmat and Pinkus 1986) employing the same idea of mixing of two streams of oil.

The hot oil carryover factor λ has been examined experimentally. Ettles and Cameron (1968) investigated the mixing temperature in a parallel plate thrust bearing. Mitsui et al (1983) conducted correlations of λ as a function of oil supply flowrate for a journal bearing. Heshmat and Pinkus (1986) presented empirical correlations for both journal and thrust bearings. Their study shows that the hot oil carryover is primarily affected by the shaft surface velocity, λ decreases with increasing velocity.

As its name suggests, the hot oil carryover factor could reflect the fact that some hot oil is lost when crossing the groove. Centrifugal force may detach some hot oil from the shaft surface. Part of the bearing's structure, such as the short land in front of the pad groove, may block some hot oil from reaching the mixing area. The cool oil jet may prevent some hot oil from reaching the downstream pad. All these mechanisms certainly can lead to a temperature that is lower than what Equation (3) predicts. However, the CFD study by Grzegorz and Michal (2007) indicates that the lower inlet temperature is largely due to intense heat convection between the hot oil layer and the cool oil in the groove. By tracking oil particles, they found that most of the oil entering the pad inlet comes from the upstream pad, most of the cool oil from the supply hole moves in a whirl across the groove. Thus, they state that "From the first results it seems that the efficiency of lubricating groove lies in intensive convective heat exchange in the lubricating groove rather than in the actual forcing fresh oil to enter the oil film." In other words, even if all of the inlet oil comes from the hot oil carryover, its temperature would still be lowered since the hot oil layer is cooled along its way across the groove.

If this is true, Equation (4) should not be interpreted as the simulation of two streams mixing. Instead, the model is basically a weighted average between two known temperatures, with λ as the weighting function that reflects the intensity of the heat transfer. Moreover, the averaging must be subject to physical constraints. As discussed above, λ=1 gives the upper limit of the mixing temperature. However, λ=0 does not necessarily give the lower limit since the amount of cool oil is finite. The lower limit can be obtained by the cool oil insertion model:

$$T_{mix} = T_{in} = \frac{(Q_{in} - Q_s) T_{out} + Q_s T_s}{Q_{in}} \quad (5)$$

This equation means that all the available supply oil is used to cool the minimum amount of hot oil in the most efficient way. If the physics is indeed mass mixing, rather than heat transfer, Equation (5) means that all supply oil enters the pad inlet, and the remaining space is occupied by the hot oil carryover, which is the opposite of Equation (3). This cool oil insertion model was used by Dmochowski *et al*. (1993) to analyze inlet groove bearings.

In reality, it is likely that both mass mixing and heat convection take place within the oil groove. Regardless of which one is dominant, Equation (4) is able to produce the measured inlet temperature. However, as the physical meaning of λ becomes vague, its determination becomes increasingly dependent on empirical correlation. Therefore, it is very important to understand what happens in the groove, and consequently develop more accurate and generally predictive models.

In this study, if the pad is not starved, Equation (4) is used to predict the groove mixing temperature as long as the result does not exceed the lower limit set by Equation (5). If the result exceeds the limit, the mixing temperature is set at the value given by Equation (5). If the pad is starved, we assumed that both hot and cool oil streams enter the pad inlet and get mixed. Thus, the mixing temperature becomes

$$T_{mix} = T_{in} = \frac{Q_{out} T_{out} + Q_s T_s}{Q_{out} + Q_s} \quad (6)$$

Without better knowledge of hot oil loss, it was assumed that all hot oil leaving the upstream pad enters the downstream pad in case of starvation. This may lead to a prediction that is higher than reality. In addition, it was assumed that the supply oil is evenly distributed among the oil grooves. For example, for a five pad bearing, Q_s in Equations (5) and (6) equals one fifth of the total supply flowrate. The same even distribution was also assumed by Brockwell et al. (1994).

In summary, the physics of groove mixing is very complex and not well understood. As practical solutions, both the classic model of Equation (4) and the cool oil insertion model of Equation (5) have been used for direct lubrication prior to this study. In this study, Equations (4), (5) and (6) are combined into an integrated model. The inlet temperature of a pad is determined by one of these three equations depending on which equation's criterion of use is met.

INVESTIGATED BEARINGS

Three directly lubricated bearings were analyzed by the theoretical models described above. The pictures of the bearing pads are shown in Figure 1. The major bearing geometry and test information are summarized in Table 1. As shown in this table, the speed and load ranges cover typical industrial applications, and the loading direction has both load on pad (LOP) and load between pad (LBP) orientations. It should be pointed out that Bearing A1 was tested with one end seal, thus,

its lubrication condition is neither flooded nor totally evacuated. In addition, since none of these bearings has the same design as that in He *et al.* (2002), the triggered turbulence theory was not applied here.

Other than their special oil supply methods, these directly lubricated bearings share the same fundamental hydrodynamic principles. Therefore, the analysis was set up in the same way as that used to analyze conventional bearings, except the hot oil carryover factor which reflects the different oil feeding methods. For instance, the elasticity model always included the pad mechanical and thermal deformations, as well as the pivot flexibility. The hot clearance was calculated based on the pad thermal deformation only, assuming complete cancellation of the shaft and shell expansion. The critical Reynolds numbers that govern the flow regime transition were fixed at 500 and 1000 respectively. The heat convection coefficient on the back of the pads remained the same throughout all analysis. Keeping such consistency is essential in examining whether the TEHD model is capable of predicting the bearings' performance.

Table 1 Summary of Investigated Bearings

Bearing Index	A1	A2	B
Source	Carter, 2009	Kulhanek, 2010	Harris, 2008
Type	Inlet Groove		Spray Bar
Diameter (in)	4.0		
No. of Pads	5		4
Axial Length (in)	2.375		4.0
Pad Arc Length (deg)	57.87		73
Dia. Assembly Clearance (in)	0.0062	0.0064	0.0075
Preload (dim)	0.282	0.27	0.37, 0.56
Pivot Offset (dim)	0.6	0.5	0.65
No. of End Seals	1	2	0
Speed Range (rpm)	4000 - 13000	7000 - 16000	4000 – 12000
Load Range (psi)	50-450		50 – 275
Load Direction	LOP	LBP	
Lubricant	ISO VG32		

RESULTS

Bearings A1 and A2

The results of bearings A1 and A2 are presented together because they have the same inlet groove design. Figures 7 to 15 plot the pad temperature distributions of Bearing A1 under a variety of speed and load conditions. The TEHD predictions generally show close agreement with the experimental data. The temperatures for Bearing A2 are compared in Figures 16 to 24, showing the same level of agreement. The consistently good agreement near the leading edge indicates that the mixing model is capable of predicting the inlet temperature. In addition, Bearing A1 has 60 percent offset pivots while A2 has center pivots. Consequently, the maximum pad temperatures for A1 should occur very close to the trailing edges while for A2, it should occur relatively upstream, farther away from the trailing edges (DeCamillo and Brockwell, 2001). As shown in these figures, The TEHD models consistently predicted such different behaviors.

For Bearing A1, which has LOP orientation, the TEHD model tends to under-predict the peak temperature of the loaded pad. As the load increases, the discrepancy becomes higher and reaches about 18 ^{o}F (10 ^{o}C). Meanwhile, shaft speed shows little influence on this discrepancy. From 7000 rpm to 13000 rpm, the largest difference between the theoretical and test values remains at approximately 18 ^{o}F (10 ^{o}C). Therefore, it is reasonable to assume that the error is mainly caused by the inaccurate modeling of the elastic deformation using the two-dimensional finite element method. The actual deformation could have significant axial variation, and thus, require a three-dimensional model. While the actual pad is thicker around the pivot, software limitations required a uniform thickness. Some of the discrepancy is also due to the fact that the shaft and shell's thermal expansion was not included in the hot clearance calculation.

TEHD modeling of Bearing A2, which has LBP configuration, shows similar close agreement with experimental data. The maximum temperature is predicted to be 18 ^{o}F (10 ^{o}C) lower than the measured for the loaded pad in the high load cases. Like Bearing A1, this discrepancy is not sensitive to the shaft speed. However, for this bearing, the under-prediction is mostly on the second loaded pad (the pad to the right of the load vector in those figures). The test results show that the second loaded pad has higher temperature compared to the first one. The theoretical model gives very symmetric distributions on both pads. The cause could be the same error in the deformation modeling. Or the two pads could be different due to the manufacturing tolerances.

The hot oil carryover factor (λ) used to produce these TEHD predictions are plotted in Figure 25. As shown in this figure, the hot oil carryover factor is clearly a function of speed. At low speeds, it falls in the same region as conventional bearings, indicating similar thermal behavior. However, λ decreases substantially as speed increases. This speed dependency not only agrees with the findings of Heshmat and Pinkus (1986), but also agrees with the industrial observation that directly lubricated bearings show more thermal advantages at higher speeds. The low inlet temperature at higher speeds may be attributed to one (or several) of the following potential mechanisms: First, more cool oil enters the clearance because it is conveniently available near the inlet. Second, with increasing centrifugal force, more hot oil is blocked by the short land region before the groove, or pushed aside by the cool oil. Third, the groove enhances convective heat transfer by placing the coolant near the hot oil and isolating it from the sump oil. It is well known that the heat convection coefficient is highly dependent on the velocity of the fluids.

Further examination of the theoretical results reveals the limitation of the simple groove mixing model, highlighting the complexity of the real physics and the need to understand it. For example, the inlet temperature of the third pad is noticeably over-predicted in Figure 24. However, the predicted inlet temperature is already at its minimum value given by the cool

oil insertion model (Equation (5)). In other words, all available cool oil has been used in the mixing, yet the predicted temperature is still higher than the measurement. First, it is possible that some hot oil is lost and the surrounding sump oil, which is much cooler, 149 °F (65 °C), participated in the mixing. Second, before reaching the inlet groove, the hot oil layer must pass the space between those two pads. Since that space is full of sump oil, significant heat exchange could take place between the hot and sump oil. Thus, the hot oil layer has been cooled before reaching the groove mixing. Moreover, the supply oil may not be evenly distributed among the orifices, and this pad could somehow receive more than one fifth of the total supply oil. Unfortunately, these theories cannot be proven or dismissed without better understanding of the actual physics. In addition, as shown in Figure 24, the cool oil insertion model would under-predict the inlet temperatures for the loaded pads, indicating the need to integrate the classic mixing model and the cool oil insertion model.

The comparisons of the journal centerline loci are presented in Figures 26 and 29. Given the uncertainties involved in locating the absolute center of the bearing, the relative journal positions (Δ_{rel}) are shown using the position of the lightest load of 50 psi (345 kPa) as the reference. Each plot demonstrates how the shaft moves from its initial position under increasing load and constant speed. As shown in these figures, the agreement between the TEHD and experimental results is consistently very good. The largest discrepancy is slightly over 10 percent in Figure 29. Although not presented here, the temperature and journal loci comparisons were also made for other speeds and loads, showing very similar trend and level of agreement.

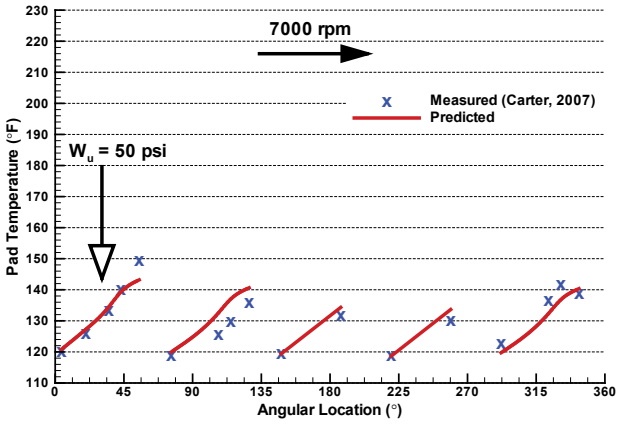

Figure 7. Pad Temperature Distributions, Bearing A1, 7000 rpm, 50 psi

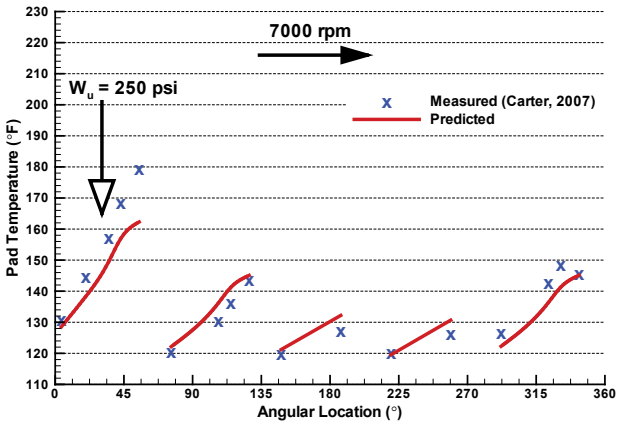

Figure 8. Pad Temperature Distributions, Bearing A1, 7000 rpm, 250 psi

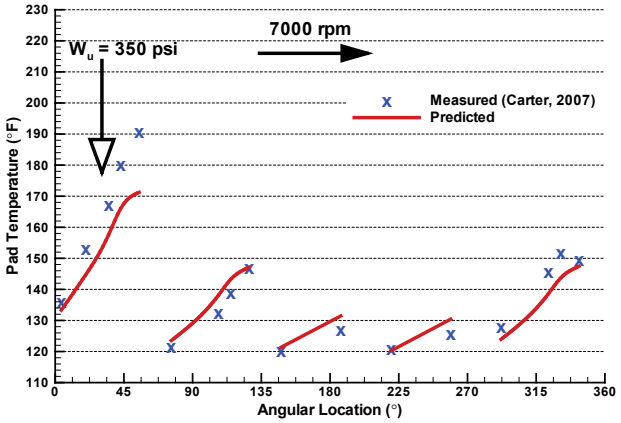

Figure 9. Pad Temperature Distributions, Bearing A1, 7000 rpm, 350 psi

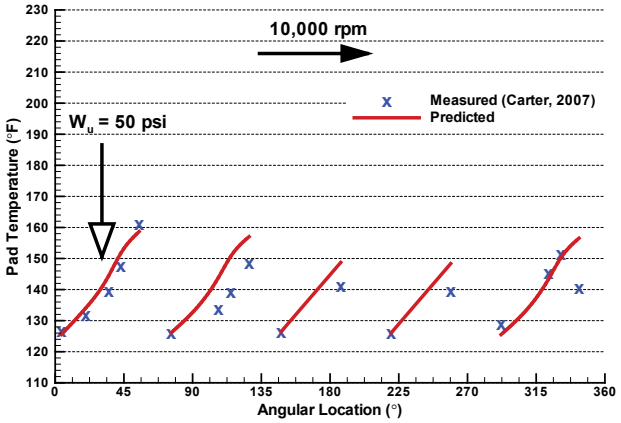

Figure 10. Pad Temperature Distributions, Bearing A1, 10000 rpm, 50 psi

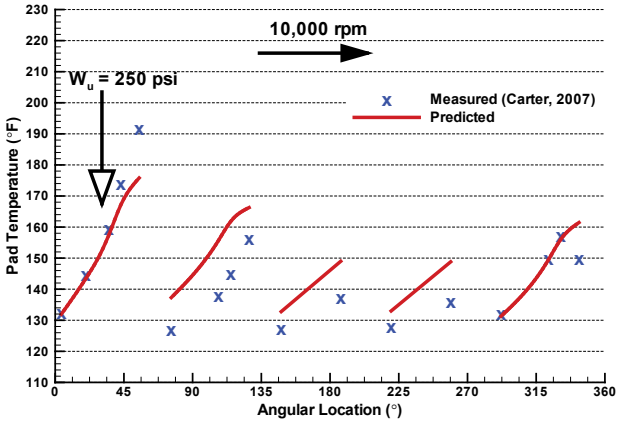

Figure 11. Pad Temperature Distributions, Bearing A1, 10000 rpm, 250 psi

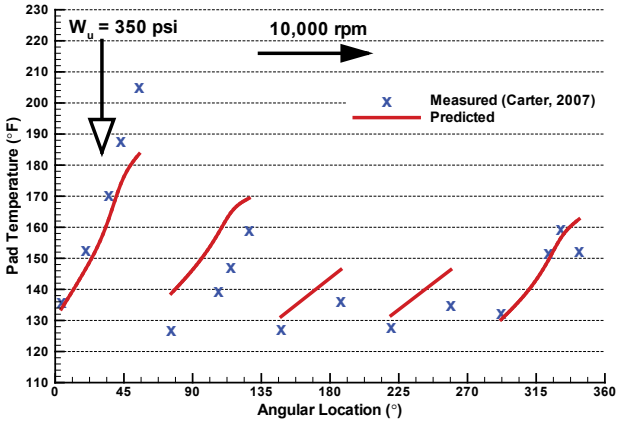

Figure 12. Pad Temperature Distributions, Bearing A1, 10000 rpm, 350 psi

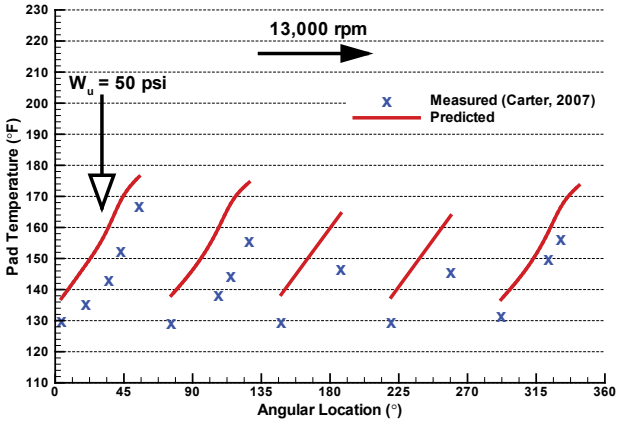

Figure 13. Pad Temperature Distributions, Bearing A1, 13000 rpm, 50 psi

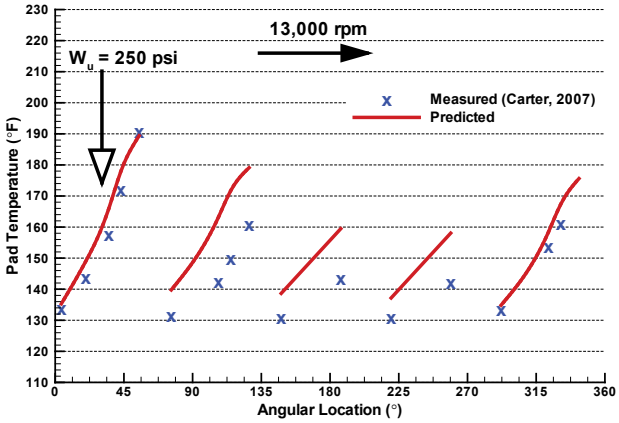

Figure 14. Pad Temperature Distributions, Bearing A1, 13000 rpm, 250 psi

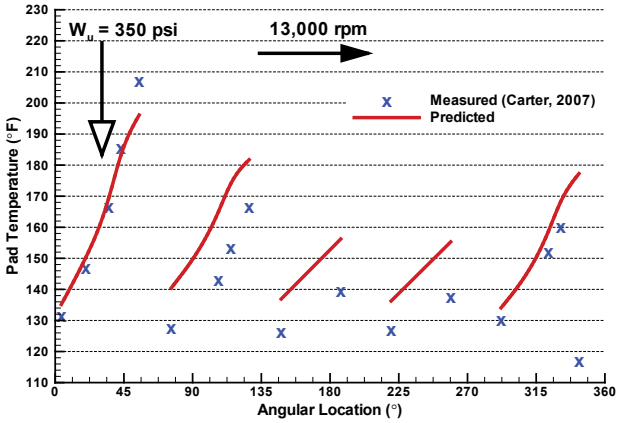

Figure 15. Pad Temperature Distributions, Bearing A1, 13000 rpm, 350 psi

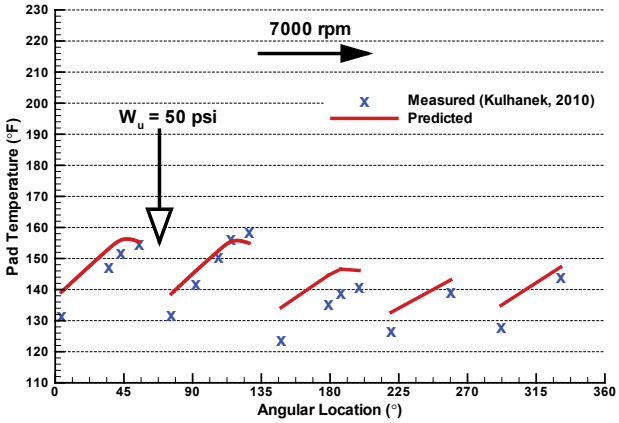

Figure 16. Pad Temperature Distributions, Bearing A2, 7000 rpm, 50 psi

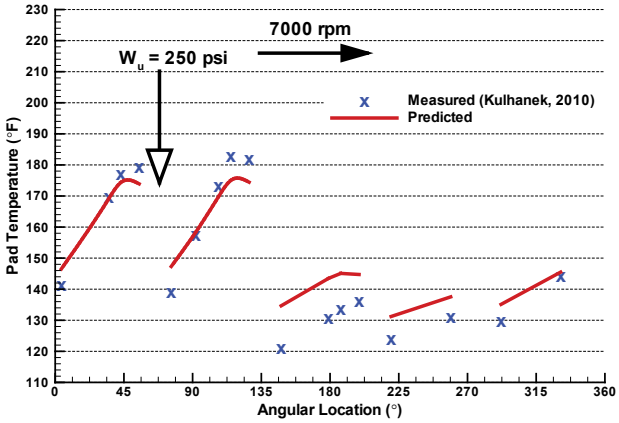

Figure 17. Pad Temperature Distributions, Bearing A2, 7000 rpm, 250 psi

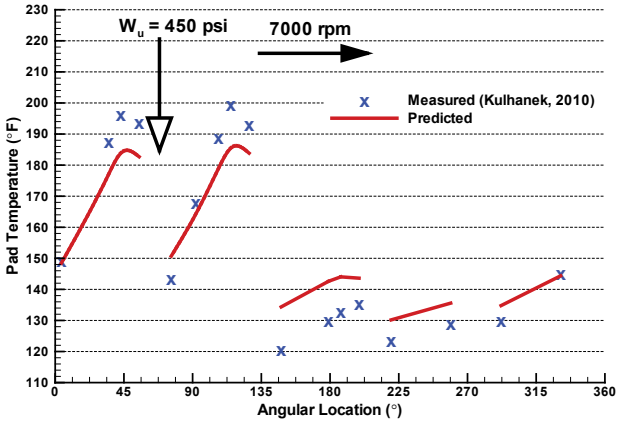

Figure 18. Pad Temperature Distributions, Bearing A2, 7000 rpm, 3103 kPa (450 psi)

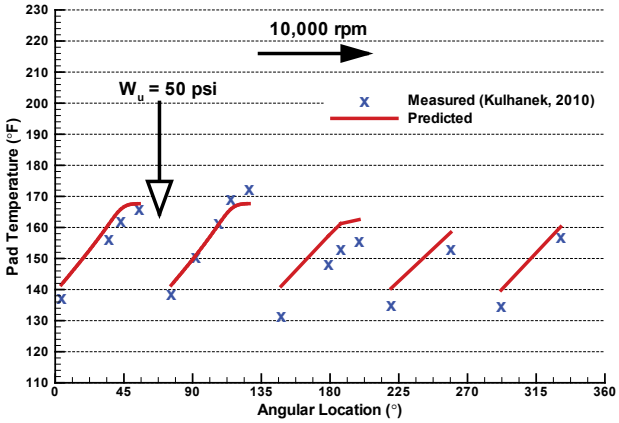

Figure 19. Pad Temperature Distributions, Bearing A2, 10000 rpm, 50 psi

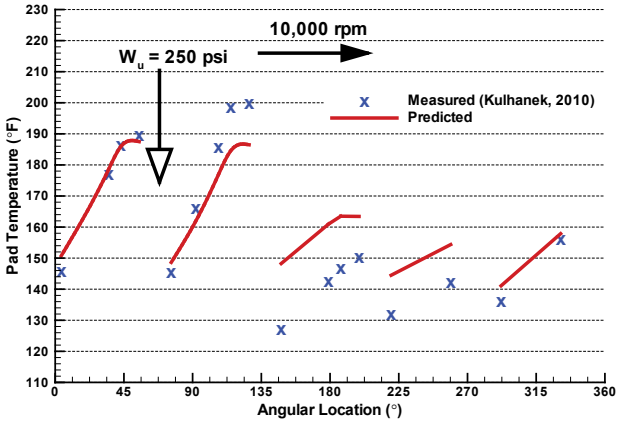

Figure 20. Pad Temperature Distributions, Bearing A2, 10000 rpm, 250 psi

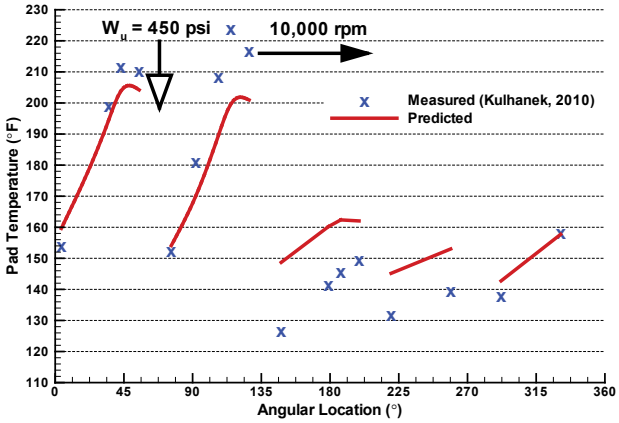

Figure 21. Pad Temperature Distributions, Bearing A2, 10000 rpm, 450 psi

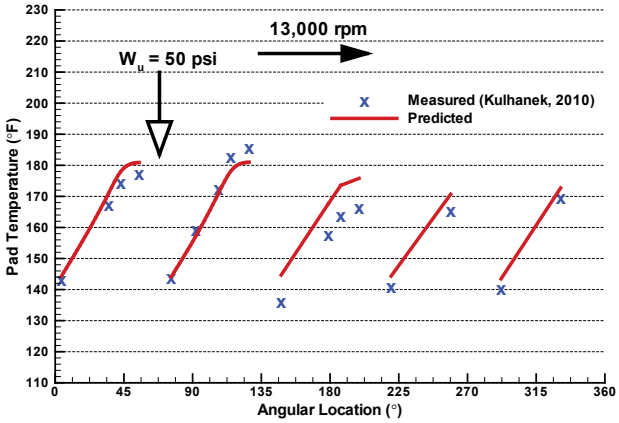

Figure 22. Pad Temperature Distributions, Bearing A2, 13000 rpm, 50 psi

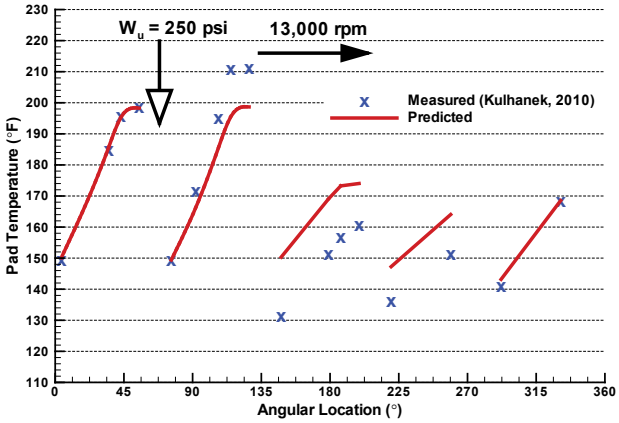

Figure 23. Pad Temperature Distributions, Bearing A2, 13000 rpm, 250 psi

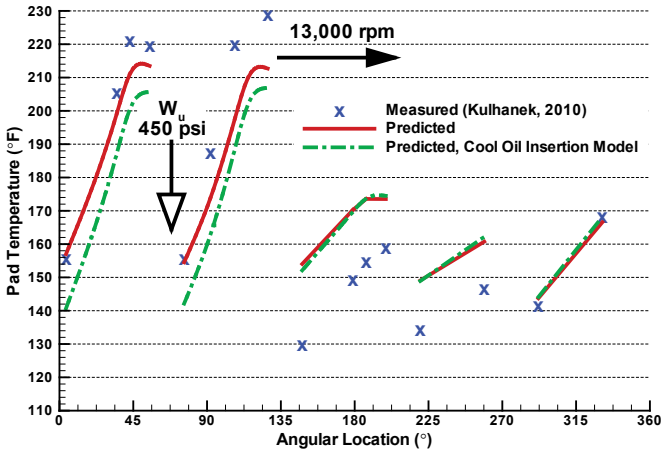

Figure 24. Pad Temperature Distributions, Bearing A2, 13000 rpm, 450 psi

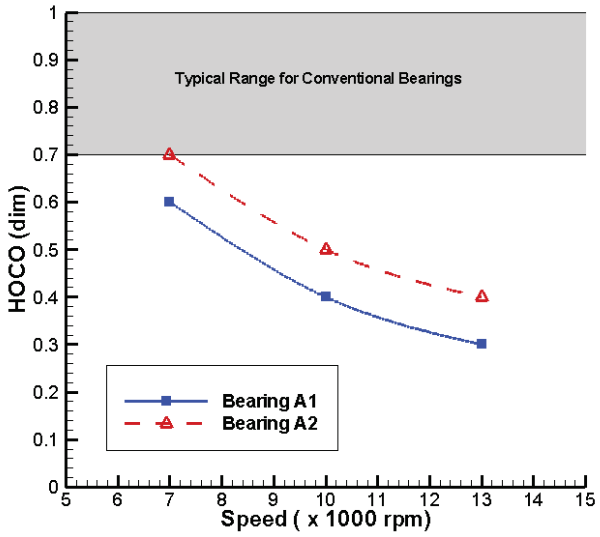

Figure 25. Hot Oil Carryover Factor (λ) versus Speed

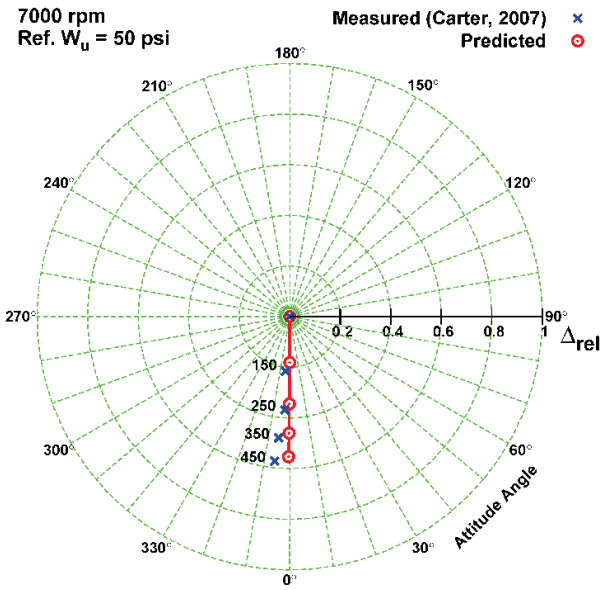

Figure 26. Journal Centerline Loci, Relative, Bearing A1, 7000 rpm

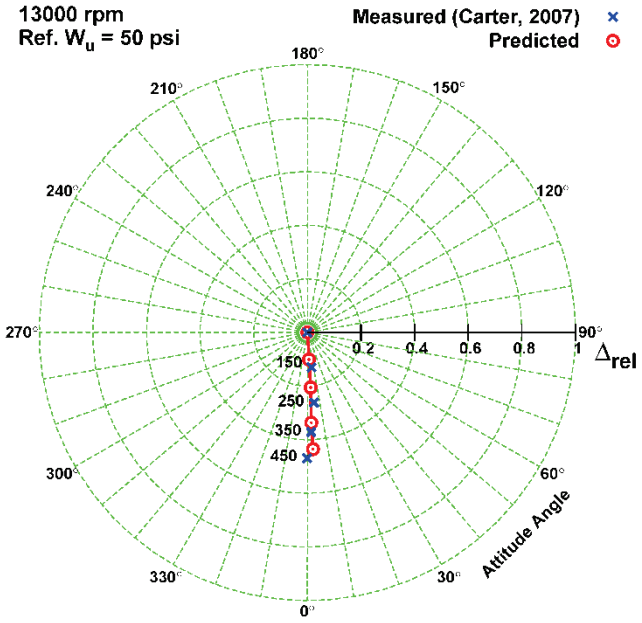

Figure 27. Journal Centerline Loci, Relative, Bearing A1, 13000 rpm

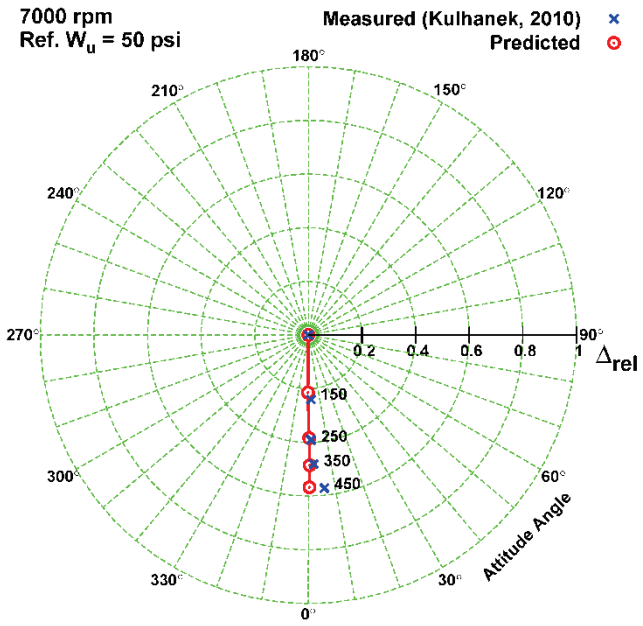

Figure 28. Journal Centerline Loci, Relative, Bearing A2, 7000 rpm

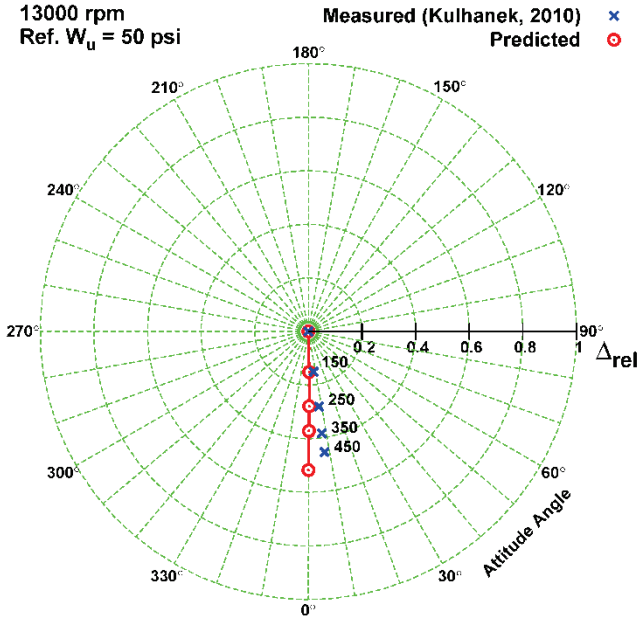

Figure 29. Journal Centerline Loci, Relative, Bearing A2, 13000 rpm

Bearing B

Bearing B feeds supply oil to the pad inlet by bars with axially distributed nozzles that point radially. The radial jets of cool oil hit the hot oil layer adhering to the shaft surface and these two streams get mixed. The flow pattern in the spray bar bearing is likely rather different from that in the inlet groove bearing. For an inlet groove bearing, the cool oil inside the groove forms vortices that are driven by the circumferentially moving hot oil layer (Heshmat and Pinkus 1986; Edney et al, 1998; Grzegorz and Michal, 2007). And thus, the shaft surface velocity has significant influence on the cool oil's flow pattern. However, the spray bar geometry is unlikely to produce such vortices, especially considering that the operation is evacuated. Nevertheless, the simple mixing model should be capable of producing the average temperature of the two streams, as long as the weighting function of λ is properly selected.

Investigating this bearing involves several additional complexities. First, each pad has only one thermocouple near its trailing edge (93 percent of the total pad arc). To assess the mixing model and determine the proper hot oil carryover factor, it is very important to have temperature measurement near the leading edge. Second, some supply oil is redirected and sprayed on the backs of the two loaded pads. This coolant is applied near the thermocouple and affects the measurements, but the current TEHD model does not include this type of local cooling. Third, this bearing is more complicated in design and construction. The pads are made of copper with a bronze insert. Circumferential grooves were cut on the backs of the pads to increase the heat exchange area. The two upper pads (Pad 1 and 2) have higher preload than the loaded pads (Pad 3 and 4). They also have chamfers at their leading edges intended to suppress pad flutter.

In addition, Harris (2008) noticed that the bearing was unevenly crushed by the instrumentation housing, leading to reduced assembly clearance on two pads (Pad 1 and 3), and enlarged clearance on the other pads (Pad 2 and 4). The pivot style is ball-in-socket, which is typically fairly stiff. However, Harris (2008) measured 2.0E+6 lbf/in (350 MN/m) structural stiffness, which is significantly lower than the pivot stiffness obtained by Hertzian contact theory. Although the exact reason for the low structural stiffness is unknown, it surely affected the bearing's performance and was included in the TEHD model.

To model the measured geometry, the analysis included different clearance and preload for each pad. The pivot stiffness was specified at the measured value of 2.0E+6 lbf/in (350 MN/m). The model also considered the inlet chamfers and material properties of copper. Since the cool oil is directly sprayed to the pad inlet, Equation (5) was used, which means all cool oil can enter the bearing clearance, and the remaining space will be filled by hot oil carryover. Obviously, this is an idealized assumption. However, due to the lack of temperature measurement near the leading edge, this idealized model was used for the current analysis as the first effort. Future study is necessary to enable better empirical correlation of λ and understanding of the physics.

The resulting temperatures under various speeds and loads are presented and compared from Figures 30 to 32. In general, the agreement is relatively good. The highest discrepancy is about 20 ^{o}F (11 ^{o}C) over-prediction on Pad 4. Since the model cannot simulate the local back cooling on Pad 3 and 4, increased discrepancies on these pads are expected.

Figures 33 to 35 show the bearing centerline loci as the function of load under three difference shaft speeds. Similar to the previous plots, the loci are shown as relative to the position of the lightest load of 50 psi (345 kPa). Although the load is vertically downward, the journal shows substantial attitude angle (horizontal displacement) as the result of the uneven crush. This unusual attitude angle is well predicted by the TEHD model. At low speed, the TEHD model predicts more centerline displacement than the experiment observed (approximate 40 percent). But the agreement improves as the

speed increases and becomes very good at 12000 rpm (within 5 percent).

It is likely that the discrepancies are mostly due to the limitations of the elastic model. Like the other bearings, the actual deformation is three-dimensional rather than two-dimensional. The actual pad has a spherical cutout to house its pivot and circumferential grooves for back cooling, while the model assumed a smooth shell with uniform thickness. In the theoretical analysis, the measured support stiffness, which represents the combined elasticity of the pivot and shell, was modeled as pivot stiffness. However in reality, the shell deformation is continuous, whose flexibility cannot be adequately represented by four discrete and independent linear springs. Therefore, modeling such complex deformations using springs with constant stiffness is an oversimplification. Moreover, the analysis assumed that the shaft and shell's thermal growth completely cancel each other, leading to additional errors in the hot clearance calculation. The importance of accurate elasticity modeling is also demonstrated in Figure 35. As shown in this figure, not including the pad and support deformations, the shaft centerline displacements are grossly under-predicted, and the attitude angle shows substantial error compared to the test data.

In addition, it was observed that some pads were starved under high speed conditions. In case of starvation, the starvation model was automatically turned on, searching the film onset location and including the subsequent effects.

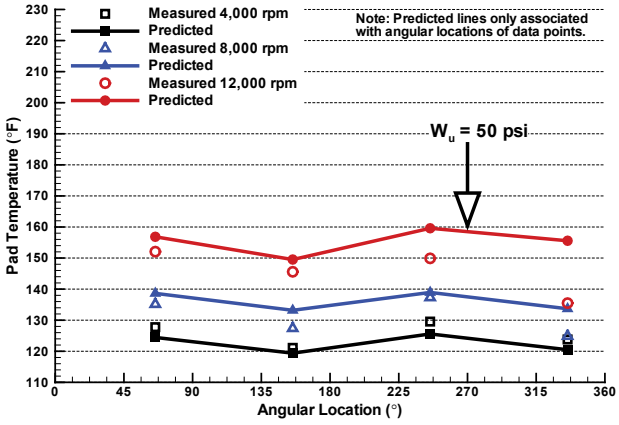

Figure 30. Pad Temperature Distributions, Bearing B, 50 psi, Varous Speeds

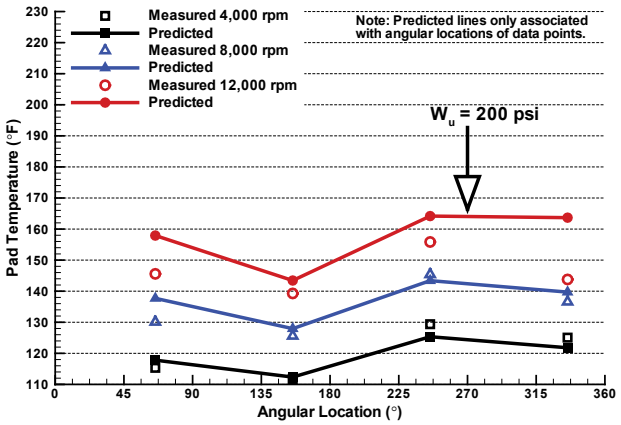

Figure 31. Pad Temperature Distributions, Bearing B, 200 psi, Varous Speeds

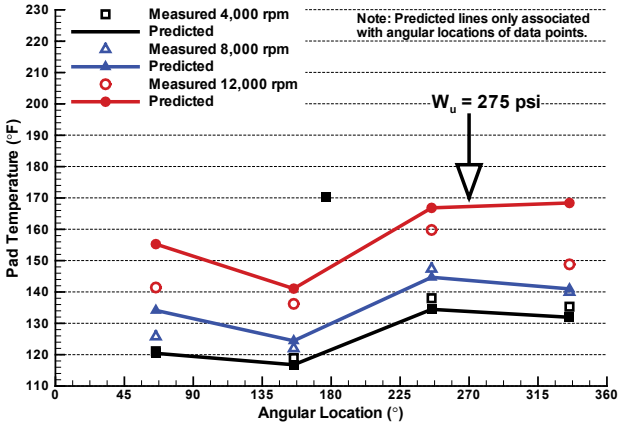

Figure 32. Pad Temperature Distributions, Bearing B, 275 psi, Varous Speeds

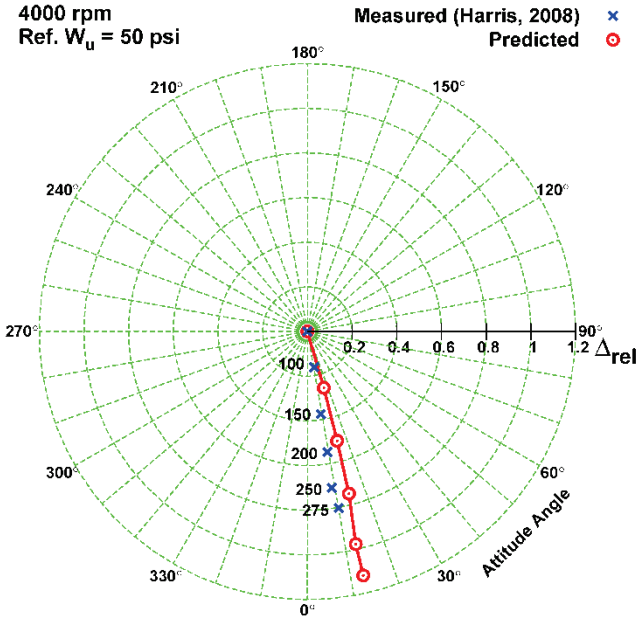

Figure 33. Journal Centerline Loci, Relative, Bearing B, 4000 rpm

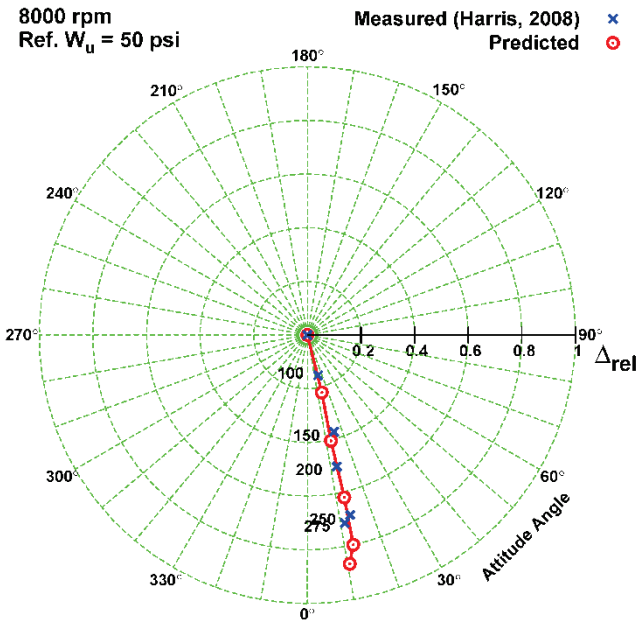

Figure 34. Journal Centerline Loci, Relative, Bearing B, 8000 rpm

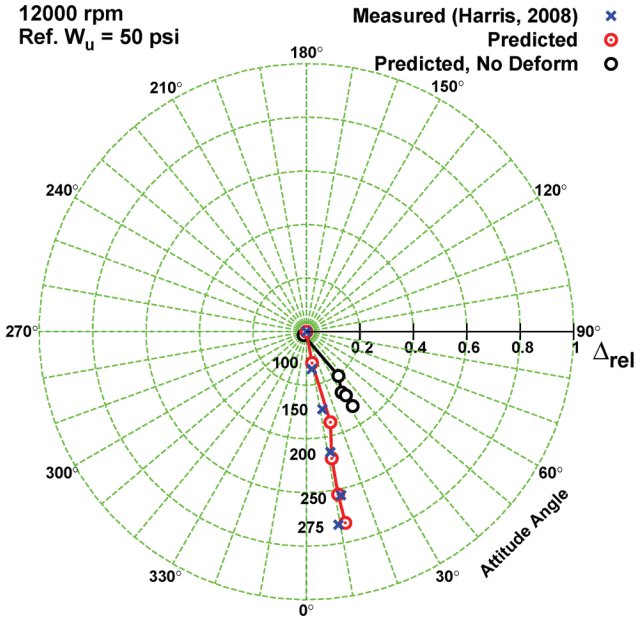

Figure 35. Journal Centerline Loci, Relative, Bearing B, 12000 rpm

CONCLUSIONS AND RECOMMENDATIONS

Studies on bearing dynamics have received considerable attention because the dynamic coefficients directly affect a machine's rotordynamic performance. However, a bearing's dynamic characteristics are fundamentally governed by its steady state behavior. The confidence in the dynamic coefficients is intrinsically dependent on the accuracy of its corresponding steady state predictions. For example, the accuracy of dynamic coefficients would be in serious question if the predicted shaft steady state operating position and/or pad temperatures were far away from the measurements.

This investigation focused on assessing the steady state predicative capabilities for some of the most complex journal bearing designs, those incorporating direct lubrication features. Revisiting the primary questions and findings of this investigation:

- *What are the state-of-the-art techniques for modeling directly lubricated journal bearing?*
  - To predict the low pad inlet temperature, there are three mixing models: the classic mixing model, the cool oil insertion model, and the integrated mixing model.
  - Triggered turbulence is another modeling approach applied to some direct lubrication designs to predict the low circumferential temperature gradient.
  - All these models represent significant simplifications to a variety of physical phenomena which are dependent on the specifics of the direct lubrication design as well as the operating conditions, such as speed, load and oil supply flowrate.
- *How well do these modeling techniques predict the steady state performance of directly lubricated bearings?*
  - Previous investigations indicated that the triggered turbulence model can achieve reasonable accuracy in predicting one type of inlet groove bearing. However, none of the bearings investigated here is of that design. Therefore, its capability was not assessed in this study.
  - For the three bearings investigated here, predictions using the integrated mixing model achieved reasonable accuracy regarding the pad temperatures and shaft centerline displacements.
    - For the two inlet groove bearings, the largest deviation is shown as the 18 ^{o}F (10 ^{o}C) under-predicted maximum temperature, which typically occurred at relatively high load ($W_U \geq 200$ psi (1379 kPa).
    - For the spray bar bearing, the largest deviation is shown in the shaft centerline prediction at the lowest speed (4000 rpm) when the unit load reached its maximum of 275 psi (1896 kPa).
    - For all three bearings, the hot oil carryover factors were much smaller than those for conventional bearings and were found dependent on operating conditions, especially speed.
  - Besides the mixing temperature, it is also very important to properly model other physical aspects. For example, without elasticity, the shaft centerline displacements of the spray bar bearing were grossly under-predicted (Figure 35). Although not significant in this investigation, starvation must be modeled if the bearing is starved in operation.
- *What are the likely causes for these deviations between predictions and measurements?*
  - For the two inlet groove bearings, the temperature errors are mainly attributed to the limitations of the elastic model, including the two-dimensional pad deformation, simplified pad geometry, and no directly modeling of the shaft and shell thermal expansions. Meanwhile, the integrated groove mixing model provides good

predictions for the loaded pads, but shows its limitations on some unloaded pads.
    - For the spray bar bearing, the errors in the relative centerline displacements can be attributed to the over-simplifications of large, complex shell/pivot deformations (mechanical and thermal) using a single pivot stiffness value.

The authors are currently investigating options to address those modeling limitations. Future efforts include CFD studies to better understand and quantify pad inlet conditions, and three-dimensional finite element modeling of the actual pad geometries. In addition, the following recommendations are provided for any future experimental work:

- Use three thermocouples across the pad's axial length at the circumferential locations of the pad leading edge, 75 percent arc length, and trailing edge.
- Measure bearing housing temperature at several locations. It is well known that a bearing's performance is significantly influenced by its hot clearance, which is established by the combined thermal growth of the journal, bearing pads and housing. Unfortunately, the journal and housing deformations are often neglected in experimental investigations. In this analytical study, the bearings' hot clearances were established by the pad thermal deformation only. The journal and housing were not modeled because their conditions were not adequately known. To address this lack of knowledge, we recommend:
    - Additional temperature measurements on the housing to help understand their thermal growth and distortions.
    - Opposing proximity probes to improve the accuracy of shaft centerline measurement and better understand the housing's distortion and thermal growth.
- Be aware of potential starvation and its influences on the test results.

NOMENCLATURE

C_p	Lubricant specific heat
G	A film viscosity function in the Reynolds equation
h	Heat convection coefficient on the pad outer surfaces
p	Pressure
q	heat flux on the pad outer surfaces
Q	Flowrate
Q_{in}	Flowrate at pad inlet
Q_{out}	Flowrate at the outlet of the upstream pad
Q_s	Oil supply flowrate to a pad
T	Temperature
T_{in}	Oil temperature at pad inlet
T_{out}	Oil temperature at the outlet of the upstream pad
T_s	Oil supply temperature
T_{mix}	Oil mixing temperature, equals T_{in}
T_a	Ambient temperature
T_{shaft}	Shaft surface temperature
u	Oil velocity in circumferential (x) direction
U	Shaft surface velocity
v	Oil velocity in radial (y) direction
W_U	Unit load
w	Fluid velocity in axial (z) direction
x	Circumferential direction along a pad
y	Radial direction across film
z	Axial direction along a pad
Δ_{rel}	Shaft centerline relative displacement
Γ	A film viscosity function in the Reynolds equation
κ	Heat conductivity
κ_e	Effective heat conductivity including turbulence
λ	Hot oil carry over factor
μ	Viscosity
μ_e	Effective viscosity including turbulence
ρ	Density
ω	Shaft rotational speed

REFERENCES

1. Brockwell, K., Dmochowski, W., and DeCamillo, S, 1994, "Analysis and Testing of the LEG Tilting Pad Journal Bearing – a New Design for Increasing Load Capacity, Reduced Operating Temperatures and Conserving Energy," *Proceedings of the Twenty-Third Turbomachinery Symposium*, Turbomachinery Laboratory, Texas A&M University, College Station, Texas, pp. 43-56.

2. Carter, C. R., 2007, "Measured and Predicted Rotordynamic Coefficients and Static Performance of a Rocker-Pivot Tilt Pad Bearing in Load-on-Pad and Load-between-Pad configurations," *Master Thesis*, Texas A&M University, College Station, Texas.

3. DeCamillo, S. and Brockwell, K., 2001, "A Study of Parameters That Affect Pivoted Shoe Journal Bearing Performance in High-Speed Turbomachinery," *Proceedings of the Thirtieth Turbomachinery Symposium*, Turbomachinery Laboratory, Texas A&M University, College Station, Texas, pp. 9-22.

4. Dmochowski, W., Brockwell, K., DeCamillo, S., and Mikula, A., 1993, "A Study of the Thermal Characteristics of the Leading Edge Groove and Conventional Tilting Pad Journal Bearings," *Journal of Tribology*, 115, pp.219-226.

5. Edney, S. L., Heitland, G. B, and DeCamillo, S., 1998, "Testing, Analysis, and CFD Modeling of a Profiled Leading Edge Groove Tilting Pad Journal Bearing," *Presented at the international Gas Turbine & Aeroengine Congress & Exhibition*, Stockholm, Sweden, June 2-5.

6. Ettles, C. and Cameron, A., 1968, "Consideration of Flow across a Bearing Groove," *Journal of Lubrication Technology*, 90, pp. 133-319.

7. Grzegorz, R. and Michal, W., 2007, "CFD Analysis of the Lubricant Flow in the Supply Groove of a Hydrodynamic Thrust Bearing Pad," *Proceedings of ASME/STLE International Joint Tribology Conference*, San Diego, California USA, October 22-24.

8. Harris, J. M., 2008, "Static Characteristics and Rotordynamic Coefficients of a Four-Pad Tilting-Pad Journal Bearing with Ball-in-Socket Pivots in Load-between-Pad Configuration," *Master Thesis*, Texas A&M University, College Station, Texas.

9. He, M., Allaire, P.E., Barrett, L. E., and Nicholas, J. C., 2002, "TEHD Modeling of Leading Edge Groove Journal Bearings," IFToMM, *Proceedings of the sixth International Conference on Rotor Dynamics*, 2, pp. 674-681.

10. He, M., Cloud, C. H. and Byrne J. M., 2005, "Fundamentals of Fluid Film Journal Bearing Operation and Modeling," *Proceedings of the Thirty-Fourth Turbomachinery Symposium*, Turbomachinery Laboratory, Texas A&M University, College Station, Texas, pp. 155-175.

11. Heshmat, H. and Pinkus, O., 1986, "Mixing Inlet Temperatures in Hydrodynamic Bearings", *Journal of Tribology*, 108, pp. 231-248.

12. Kirk, R. G. and Reedy, S. W., 1988, "Evaluation of Pivot Stiffness for Typical Tilting-Pad Journal bearing Design," *Journal of Vibration, Acoustics, Stress, and Reliability in Design*, 110, pp. 165-171.

13. Kulhanek, C. D., 2010, "Dynamic and Static Characteristics of a Rocker-Pivot, Tilting-Pad Bearing with 50% and 60% Offsets," *Master Thesis*, Texas A&M University, College Station, Texas.

14. Martin, F. A. and Garner, D. R., 1973, "Plain Journal Bearings under Steady State Loads: Design Guidance for Safe Operation," *First European Tribology Congress*, pp. 1-16.

15. Mikula, A. M., 1985, "The Leading-Edge-Groove Tilting-Pad Thrust Bearing: Recent Developments," *Journal of Tribology*, 107, pp.423-430.

16. Mikula, A. M., 1988, "Further Test Results of the Leading-Edge-Groove (LEG) Tilting Pad Thrust Bearing," Journal of Tribology, 110, pp.174-180.

17. Mitsui, J., Hori, Y., and Tanaka, M., 1983, "Thermohydrodynamic Analysis of Cooling Effect of Supply Oil in Circular Journal Bearing," *Journal of lubrication Technology*, 105, pp.414-421.

18. Newkirk, B. L. and Tayler, H. D., 1925, "Shaft Whipping Due to Oil Action in Journal Bearings," *General Electric Review*, 28, pp. 559-568.

19. Paranjpe, R. S., and Han, T., 1994, "A Study of the Thermohydrodynamic Performance of Steadily Loaded Journal Bearings," *Tribology Transactions*, 37, pp. 679-690.

20. Pinkus, O., 1987, "The Reynolds Centennial: a Brief History of the Theory of Hydrodynamic Lubrication," *Journal of Tribology*, 109, pp. 2-20.

21. Safar, Z. and Szeri, A. Z., 1974, "Thermohydrodynamic Lubrication in Laminar and Turbulent Regimes," *Journal of Lubrication Technology*, 96, pp. 48-56.

22. Sasaki, T., Mouri, Y., Takahashi, S., and Matsumoto, I., 1987, "Performance Improvement of Bearings in Mechanical Drive Steam Turbine by Direct Lubrication," *Mitsubishi Heavy Industry, Ltd. Technical Review*, 24, pp. 202-206.

23. Suganami, T., and Szeri, A. Z., 1979, "A Thermohydrodynamic Analysis of Journal Bearings", *Journal of Lubrication Technology*, 101, pp. 21-27.

24. Szeri, A. Z., 1987, "Some Extensions of the Lubrication Theory of Osborne Reynolds," *Journal of Tribology*, 109, pp. 21-36.

ACKNOWLEDGEMENTS

The authors would like to thank Mr. Chris Kulhanek (Southwest Research Institute) for providing necessary information that allowed this theoretical investigation. The authors would also like to thank Texas A&M University and the work of Professor Dara Childs and his former graduate students Mr. Harris, Mr. Carter, and Mr. Kulhanek for publishing the test data that were used as the basis for this work.